International Journal of Thermophysics, Vol. 21, No. 3, 2000

Nonequilibrium Molecular Dynamics Simulations of Shear Viscosity: Isoamyl Alcohol, *n*-Butyl Acetate, and Their Mixtures

Y. Yang,[1] T. A. Pakkanen,[2] and R. L. Rowley[1, 3]

Received May 26, 1999

Nonequilibrium, NVT, molecular dynamics (NEMD) simulations were used to obtain the shear viscosity, η, of isoamyl alcohol, *n*-butyl acetate, and their binary mixtures at 35°C and 0.1 MPa. The fluids were modeled using rigid bonds, rigid bond angles, appropriate torsional potentials, pairwise-additive Lennard–Jones dispersion interactions between united-atom sites, and partial point charges located at atomic centers. Simulations were performed at different shear rates, γ, and values obtained at $\gamma = 0$ are compared to experimental values. Two methods are commonly used to extrapolate pure-fluid simulated data to zero shear, $\eta(0)$. The applicability of these two methods to mixtures of polar fluids was examined in this study. It was found that linear extrapolation with respect to $\gamma^{1/2}$ can lead to ambiguous $\eta(0)$ results for some mixtures because of a curvature in the data that shows no observably distinct change in rheology. On the other hand, a log–log plot of $\eta(\gamma)$ versus γ is consistently very linear with a distinct change from shear-thinning to Newtonian rheology at lower shear rates. The latter method is recommended for consistency sake, even though agreement between experiment and $\eta(0)$ values was better with the former method. This agreement was 12 and 21% for the two methods, respectively. A negative bias in the simulated values is attributable to the united-atom model.

KEY WORDS: binary mixtures; isoamyl alcohol; *n*-butyl acetate; nonequilibrium molecular dynamics; shear viscosity; zero-shear viscosity.

[1] Department of Chemical Engineering, Brigham Young University, Provo, Utah 84602, U.S.A.
[2] Department of Chemistry, University of Joensuu, Joensuu, Finland.
[3] To whom correspondence should be addressed.

0195-928X/00/0500-0703$18.00/0

1. INTRODUCTION

Accurate methods for predicting shear viscosity of a wide range of fluids and their mixtures are not available. Although methods based on group contributions, corresponding states, significant structure theory, and empirical correlations have had considerable success, none has adequately captured the relationship between molecular structure and intermolecular interactions required to produce an accurate predictive method for pure fluids and mixtures over a range of temperatures and densities. Molecular simulations seem capable of providing this connection between molecular structure and fluid viscosity. In particular, the accuracy of viscosity values obtained from nonequilibrium molecular dynamics (NEMD) simulations is limited only by the efficacy of the model(s) used to describe the geometry and intermolecular interactions and by the method used to extrapolate simulated viscosities to zero shear. The simulations themselves accurately account for all the physics underlying the relationship between fluid structure and the molecular interactions for a given shear rate. Unfortunately, applied shear rates in NEMD simulations are very large relative to those applied in experimental studies, and so some method of extrapolating results from high shear rates to essentially zero shear is required for direct comparison of simulated and experimental viscosities. The two issues of appropriate models and extrapolation procedure are therefore key to development of NEMD simulations for use as predictive tools.

Considerable work has been done with regard to the first issue, the efficacy of various intermolecular potential models, for certain types of fluids. Many NEMD simulations of *n*-alkanes have been performed [1–4], and the agreement between simulated and experimental viscosities is generally very good, usually within 15%. Generally, the models used in these simulations include pairwise additive Lennard–Jones (LJ) interactions for the dispersion forces between sites located at atomic nuclei, torsional potentials for each group of four atoms within the molecule, and either rigid bonds or harmonic vibrational potentials. If rigid bonds are used, then bond lengths and angles are fixed at their optimum locations as determined from experiment or *ab initio* geometry optimization. To reduce the number of LJ interactions, hence the required simulation CPU time, $-CH_x$ groups are often treated as a single, united-atom (UA) interacting site. Alternatively, hydrogen atoms are explicitly included as separate interacting sites in all-atom (AA) models. Homogeneous UA models, in which all $-CH_x$ sites are equivalent, have been shown to be reasonably accurate for simulating the viscosity of *n*-alkanes, for example, *n*-butane, *n*-decane, *n*-eicosane, and *n*-hexadecane [1–4]. While homogeneous UA models have also been used to simulate the viscosity of some branched and cyclic

molecules [5–7] such as isobutane, 5-butylnonane, tridecane, and cyclohexane, better accuracy is generally obtained for such fluids when heterogeneous UA models are used. Such studies include viscosity simulations for *n*-decane, *n*-hexadecane, *n*-tetracosane, 8-*t*-butyl-hexadecane, 6-methylnonadecane, 3-methylhexane, and several others [8–11]. Simulated results for the viscosity of these fluids are often in good quantitative agreement with experimental values, but there appears to be considerable decay in the accuracy with increased branching [12].

For polar molecules, long-range Coulombic potentials must also be included in the intermolecular model. This is commonly done using partial point charges located at atomic centers. The Ewald sum method [13, 14] is an accurate and efficient means of treating these long-range interactions for small periodic systems. While potential truncation has also been used for polar fluids, the cutoff contribution to the viscosity can be significant unless large systems are used [14]. There has not been a great number of simulations performed on the viscosities of polar fluids. Simulated viscosities for water, acetone, propylchloride, formamide, dimethyl formamide, and methanol were observed to be in good agreement with the experimental values [15–18].

Simulations of accurate viscosities of polar mixtures have only recently been conducted, and then only for quite small molecules. However, results of such studies have been encouraging. For example, very good agreement with experimental viscosities was obtained from simulations on binary and ternary liquid mixtures of water, methanol, and acetone [18]. Even though a standard combining rule for the cross interactions was used, the simulated mixture viscosities exhibited maxima at the appropriate compositions, and quantitative agreement with experimental values was very good. Most of the error associated with those simulations was directly attributable to the inadequacy of the pure water model.

With respect to the second issue, that of obtaining the NEMD value of the viscosity at low enough shear for direct comparison to experiment, there is yet considerable debate on the appropriate method for extrapolation to zero shear. Viscosities, η, are generally simulated at four or five shear rates, γ, within a shear-thinning regime, and the resultant $\eta(\gamma)$ values are extrapolated to $\gamma = 0$. Unfortunately there is no known rigorous way to perform this extrapolation. Common practice has been to plot $\eta(\gamma)$ vs $\gamma^{1/2}$, which often results in linear behavior. However, more recent studies at lower shear rates indicate that there may be a Newtonian region at very low shear rates from which $\eta(0)$ can be directly obtained as either the value at the lowest γ [10] or the average of several values in the Newtonian region [18]. Unfortunately, the uncertainty in simulated values of η increases exponentially at lower shear rates, and it is often difficult to

distinguish with any degree of certainty when the plateau in the $\eta(\gamma)$ data is reached. Additional extrapolation methods [3] have been proposed, but most researchers now use one of the two methods just described. However, we know of no study of the viability of these extrapolation methods for mixtures of polar fluids.

In the present work, viscosities of model fluids representing isoamyl alcohol (IAA), *n*-butyl acetate (NBA), and their mixtures were obtained from NEMD simulations at 35°C and 0.1 MPa. The above-mentioned two extrapolation methods were used to obtain $\eta(0)$ values for comparison to experimental data. The purpose in so doing is twofold: to investigate the accuracy of simulated viscosities using simple models for mixtures of branched, polar molecules and to examine the applicability of these two extrapolation methods for mixtures of polar compounds. In so doing, we have also extended previous work on mixtures of polar molecules to larger molecules.

2. SIMULATION METHODOLOGY

2.1. Molecular Models

Heterogeneous, UA, pairwise-additive, site–site intermolecular potential models were used to model intermolecular interactions. Pair interactions consisted of combined LJ and Coulombic interactions, both located at atomic centers, in the form

$$u_{ij} = 4\varepsilon_{ij}\left[\left(\frac{\sigma_{ij}}{r_{ij}}\right)^{12} - \left(\frac{\sigma_{ij}}{r_{ij}}\right)^{6}\right] + \frac{q_i q_j}{r_{ij}} \tag{1}$$

All atoms except hydrogen atoms attached to carbon atoms were treated as interacting centers; $-CH_x$ groups were treated within the UA framework, using different LJ parameters for different x (heterogeneous UA). Model parameters used in this work are shown in Table I along with the site numbers used throughout this paper to describe the models. Bond lengths were fixed at their equilibrium value as determined from a geometry optimization using Spartan and HF/STO-3G *ab initio* calculations. For IAA, both the LJ parameters and the partial charges, q_i, were obtained from the literature [19]. The LJ paramters for NBA were obtained from the literature [20], but the q_i were calculated using the electrostatic potential method in Spartan. Table II lists the optimized bond distances and angles used.

Table I. Intermolecular Site–Site Parameters Used in the Simulations

Molecule	Site No.	Site	ε/k (K)	σ (Å)	q (esu)
Isoamyl alcohol	1	CH_3(–CH)	80.52	3.905	0
	2	CH_3(–CH)	80.52	3.905	0
	3	CH	59.38	3.905	0
	4	CH_2(–CH)	59.38	3.905	0
	5	CH_2(–O)	59.38	3.905	0.265
	6	O	85.55	3.07	−0.700
	7	H	0	0	0.435
n-Butyl acetate	1	CH_3(–C)	80.57	3.91	−0.145
	2	O(=C)	105.75	2.96	−0.466
	3	C	52.873	3.75	0.838
	4	O(–C)	85.6	3.00	−0.466
	5	CH_2(–O)	85.6	3.80	0.233
	6	CH_2(–CH_2)	59.42	3.905	−0.015
	7	CH_2(–CH_3)	59.42	3.905	0.067
	8	CH_3	88.12	3.905	−0.048

The only intramolecular potential to be included was the torsional potential, mathematically represented by

$$u_{\text{tors}}(\varphi)/k = \sum_{i=0}^{5} a_i \cos^i \varphi \tag{2}$$

where ϕ is the torsional angle and a_i are coefficients in the cosine series shown. The latter coefficients were obtained from the literature for dihedral

Table II. Model Bond Lengths and Angles

IAA bond distances (Å)							
1–3	1.5460	2–3	1.5460	3–4	1.5512	4–5	1.5517
5–6	1.4353	6–7	0.9913				
IAA bond angles (deg)							
1–3–2	110.29	1–3–4	110.03	2–3–4	112.33	3–4–5	113.90
4–5–6	112.55	5–6–7	103.94				
NBA bond distances (Å)							
1–3	1.5389	2–3	1.2157	3–4	1.3933	4–5	1.4402
5–6	1.5451	6–7	1.5444	7–8	1.5408		
NBA bond angles (deg)							
1–3–2	126.25	1–3–4	110.45	2–3–4	123.29	3–4–5	112.51
4–5–6	107.89	5–6–7	111.80	6–7–8	112.25		

Table III. Torsional Potential Parameters for Eq. (2)

Dihedral angle	a_0	a_1	a_2	a_3	a_4	a_5
4–5–6–7 (IAA)	851.9752	2234.713	196.2326	−3460.18	47.51213	134.2476
All others	1116	1462	−1587	−368	3156	−3788

angles associated with straight-chain groups [6, 22], but the a_i for the branched portion of IAA (involving sites 4–5–6–7 as defined in Table I) were regressed from energies of various configurations, calculated using the molecular mechanics model MM2 in Hyperchem. The resultant values of a_i, as well as the values obtained from the literature, are shown in Table III.

The repulsive part of the LJ potential (r^{-12}) was truncated at $r = 20$ Å, and long-range corrections, though insignificant, were treated in the usual way (by calculating the property correction from the cutoff to infinity with the radial distribution function set to unity). The attractive part of the LJ potential (r^{-6}) and the long-range Coulombic interactions were both handled using the Ewald sum method. Details of this approach have been previously reported [18]. Cross LJ parameters ($i \neq j$) were treated in the manner used by Wheeler and Rowley [18] in which a geometric mean is used for ε, a geometric mean is used for σ_{ij} for the r^{-6} portion of the potential, and a hybrid between the geometric and arithmetic means, $\sigma_{ij} = (\sigma_{ij}^{G} + \sigma_{ij}^{A})^{1/2}$, is used for the r^{-12} portion of the LJ potential. This method has been shown to produce a cross potential model somewhat similar to the Lorentz–Berthelot (LB) equations, but without the computational cost that LB combining rules would produce in the Ewald sum method.

2.2. Simulation Details

The NEMD simulations were performed using a NVT ensemble with a fourth-order correct predictor–corrector numerical integration scheme. It employed the SLLOD equations of motion [21] in combination with Lees–Edwards "sliding-brick" boundary conditions to generate Couette flow. Temperature was held constant using a Gaussian thermostat applied to molecular centers of mass. Bond lengths and angles were fixed using Gaussian mechanics [22] to maintain a constant distance between bonded sites and next-nearest neighbors.

Pure IAA, pure NBA, and nine mixture compositions were simulated using 300 molecules. The time step for each simulation was chosen so that the root-mean-square local displacement of molecules was 0.7 pm per time

Table IV. $\eta(0)$ Values Obtained Using Eq. (5) and Eq. (7) in Comparison to Experimental Values

Mole fraction NBA	ρ (kmol · m^{-3})	η_{exp} (mPa · s), [24]	$\eta(0)$ (mPa · s), Eq. (5)	% error, Eq. (5)	$\eta(0)$ (mPa · s), Eq. (7)	% error, Eq. (7)
0.0000	9.069	2.753	3.08	11.7	3.17	15.0
0.0998	8.915	2.631	2.75	4.4	2.51	−4.6
0.2003	8.753	2.091	2.08	−0.6	1.98	−5.2
0.3001	8.591	1.715	1.67	−2.9	1.44	−15.9
0.3999	8.430	1.418	1.26	−11.5	1.04	−26.9
0.4998	8.268	1.221	0.96	−21.3	0.84	−31.6
0.5999	8.107	1.079	0.78	−27.5	0.70	−34.8
0.6997	7.945	0.917	0.62	−32.2	0.56	−39.0
0.8002	7.783	0.811	0.68	−16.8	0.58	−29.0
0.9002	7.621	0.734	0.72	−1.6	0.64	−13.1
1.0000	7.452	0.604	0.58	−4.7	0.50	−17.9

step; it ranged from 2.38 to 2.73 fs. At each composition, a series of NEMD simulations was performed at shear rates from 2 to 225 ps^{-1}. All simulations utilized a standard multiple-time step algorithm [13], with six short steps per full step. Simulation lengths ranged from 120,000 to 400,000 time steps beyond equilibration. Equilibration duration depended upon the starting configuration. Generally simulations were initiated from a lattice structure at a lower density. During the equilibration portion of the simulation, the cell length was gradually decreased until the density reached the desired value. Pure component densities at 1 atm and 35°C were obtained from the DIPPR database [23], and the desired mixture densities were calculated using the assumption of ideal mixing. These values are listed in Table IV. Once the system was at the appropriate density, 10,000 additional time steps were used to equilibrate the system further with the applied shear before collecting data.

2.3. Viscosity at Zero Shear

As mentioned, one of the two objectives of this work was to examine the applicability of methods that have been commonly used to obtain $\eta(0)$ from $\eta(\gamma)$ data for nonpolar, pure fluids to mixtures of polar fluids. Because the previous methods are not based on rigorous theory, their applicability to mixtures containing both polar interactions and branched molecular geometry is unclear. Previous studies on nonpolar pure fluids have based the extrapolation of shear dependent viscosities to zero shear on one of the following methods [3]:

$$\eta = \eta(0) - A\gamma \tag{3}$$

$$\eta = \eta(0) - A\gamma^2 \tag{4}$$

$$\eta = \eta(0) - A\gamma^{1/2} \tag{5}$$

$$\frac{1}{\eta} = \frac{1}{\eta(0)} - A\gamma^{1/2} \tag{6}$$

$$\eta = \begin{cases} \eta(0) & \text{Newtonian region} \\ A\gamma^{\mathbf{B}} & \text{Shear-thinning region} \end{cases} \tag{7}$$

where γ is the applied shear rate. Equations (5) and (7) have emerged as the standard methods for extrapolating NEMD results to zero shear. While Eq. (7) assumes that the rheology of the fluid becomes Newtonian at a low shear rate, identification of this Newtonian plateau is very difficult, requiring large systems and long simulation times. This is because of the high signal-to-noise ratio that occurs when the shear becomes small and the response becomes as small as the statistical errors within the simulation. Generally this plateau is found by plotting $\eta(\gamma)$ values on a log–log plot and picking off the break point where the rheology changes between shear-thinning and Newtonian.

On the other hand, it has been observed that simulation results produce a straight line in the shear-thinning region when plotted in accordance with Eq. (5), and that the extrapolated values are often in good agreement with experimental data. Moreover, the results from Eq. (7) are often lower than those obtained from Eq. (5), so the extrapolation method does matter. Unfortunately, the shear rate at which the Newtonian plateau occurs depends upon the molecule, and no general method of predicting where it occurs exists, although Cui et al. [10] have shown evidence that the change in rheology may be related to the rotational relaxation time of the molecule. The systematic occurrence of Newtonian plateaus in mixtures has not been investigated to our knowledge.

In this work, simulations were performed in the shear-thinning regime to investigate the extrapolation capability of Eq. (5) for mixtures. Longer simulations were also performed at lower shear rates to identify the Newtonian plateau in accordance with Eq. (7). A comparison of the analysis methods was also performed, and simulation results from the two analysis methods were compared to experimentally determined viscosities. In using Eq. (5), a weighted least-squares analysis was performed to find $\eta(0)$. Weights were computed from the variance of the $\eta(\gamma)$ data as determined from simple block averages of 10,000 time steps each.

3. RESULTS

3.1. The Rheology of Pure Isoamyl Alcohol and *n*-Butyl Acetate

Results of the simulations for pure IAA are shown in Fig. 1. Figure 1A utilizes Eq. (5) to analyze the data, and Fig. 1B uses Eq. (7) on a log–log plot to analyze the same data. It is obvious from Fig. 1A that there is no distinct linear range in accordance with Eq. (5) that would provide a unique value of $\eta(0)$. Normally in analyzing $\eta(\gamma)$ data in this manner, it is recognized that the noise at low shear rates precludes their use in the data and that the shear-thinning rheology changes back to Newtonian at even

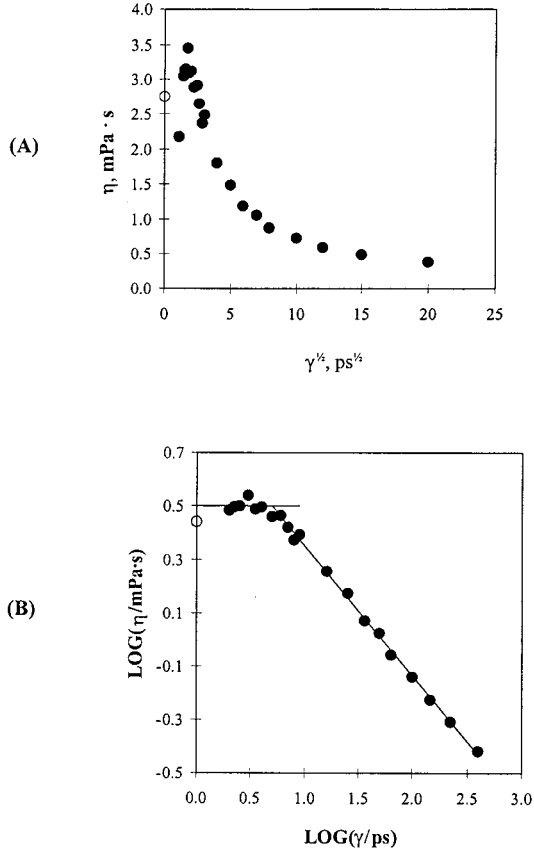

Fig. 1. Simulated viscosities (●) of IAA at 35°C and 0.1 MPa, analyzed using (A) Eq. (5) and (B) Eq. (7) and compared to the experimental value (○).

higher shear rates [1, 2]. Therefore, intermediate shear rates would be probed, say $5\ ps^{-1} \leqslant \gamma^{1/2} \leqslant 12\ ps^{-1}$, and these would be used in conjunction with Eq. (5). However, the data in Fig. 1A are not linear within the uncertainty of the data even in the $5\ ps^{-1} \leqslant \gamma^{1/2} \leqslant 12\ ps^{-1}$ range. If the data within this range are analyzed using Eq. (5), the value of $\eta(0)$ is very close to the experimental one, but the agreement seems fortuitous and dependent upon the selected points. It is clear that simulated viscosities for this fluid form a continuous curve rather than a straight line when plotted against $\gamma^{1/2}$. As can be seen in Fig. 1B, a transition between the shear-thinning and the Newtonian regions around $\gamma = 5\ ps^{-1}$ can be identified. The $\eta(0)$ value found in accordance with Eq. (7) by using a weighted average of viscosities in the Newtonian region is $3.17\ mPa \cdot s$, about 15% higher than the experimental value.

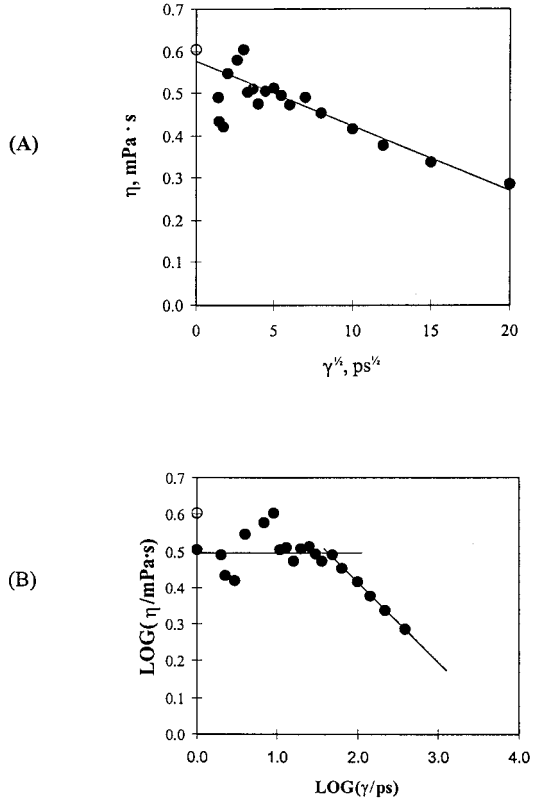

Fig. 2. Simulated viscosities (●) of NBA at 35°C and 0.1 MPa, analyzed using (A) Eq. (5) and (B) Eq. (7) and compared to the experimental value (○).

On the other hand, Fig. 2A shows that Eq. (5) describes $\eta(\gamma)$ reasonably well for NBA and does produce a value within 5% of the experimental value. There is still a slight curvature to the data, but the linear correlation is much better than for IAA. Using Eq. (7) to analyze the data produces a value for $\eta(0)$ that is 18% lower than the experimental value, but the plateau appears to be rather distinct at about 43 ps^{-1}. While the disagreement between the experimental value and the $\eta(0)$ value is certainly attributable to inadequacies in the model (e.g., rigid bonds, UA assumption, and combining rules for cross interactions), the molecule-

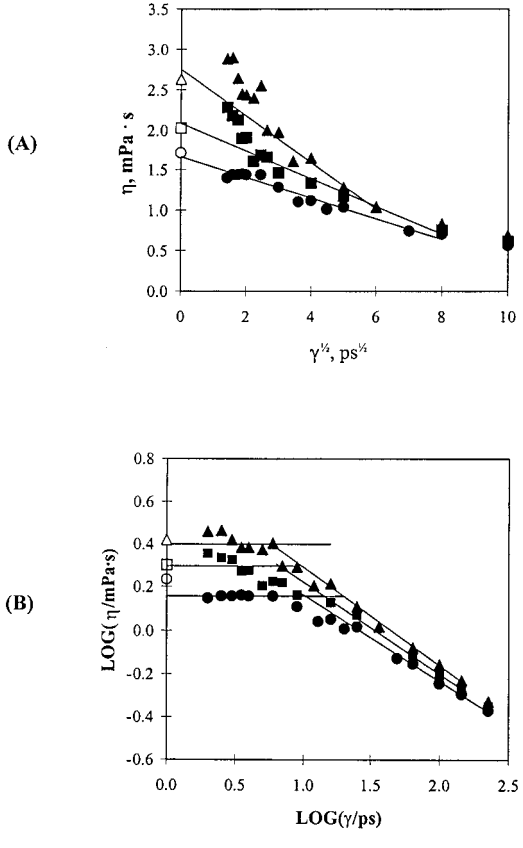

Fig. 3. Simulated viscosities of mixtures containing 10 mol% NBA + 90 mol% IAA (▲), 20 mol% NBA + 80 mol% IAA (■), and 30 mol% NBA + 70 mol% IAA (●) at 35°C and 0.1 MPa, as analyzed using (A) Eq. (5) and (B) Eq. (7) and compared to the experimental values (corresponding open symbols).

dependent deviation of $\eta(\gamma)$ from Eq. (5) linearity suggests that Eq. (7) may be the more consistent, reliable, and theoretically based method of analysis.

3.2. The Rheology of Isoamyl Alcohol and *n*-Butyl Acetate Mixtures

Figures 3–5 show the mixture results obtained from the simulations analyzed using Eqs. (5) and (7). For the compositions rich in IAA (Fig. 3), the curvature of the simulated data observed for pure IAA persists when Eq. (5) is used to extrapolate to zero shear. When the same data are

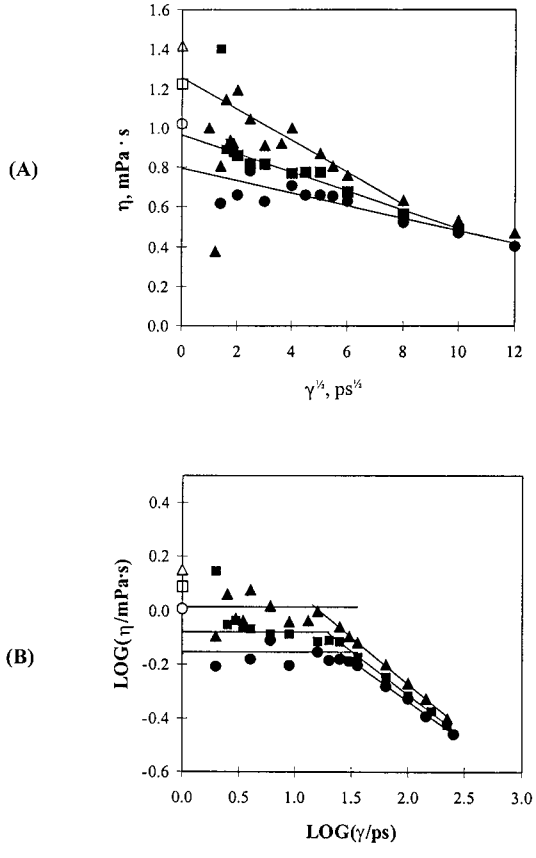

Fig. 4. Simulated viscosities of mixtures containing 40 mol% NBA + 60 mol% IAA (▲), 50 mol% NBA + 50 mol% IAA (■), and 60 mol% NBA + 40 mol% IAA (●) at 35°C and 0.1 MPa, as analyzed using (A) Eq. (5) and (B) Eq. (7) and compared to the experimental values (corresponding open symbols).

analyzed in terms of Eq. (7), definite breaks in the rheology are observed and the Newtonian viscosity can be obtained in spite of the larger scatter at low γ. Both analyses produce reasonably good agreement with experimental measurements. The results for mixtures that contain roughly equal molar amounts of the two components (Fig. 4), appear to be more linear with respect to Eq. (5) than mixtures richer in IAA, but it is difficult to tell where the linear region begins and ends. This makes the extrapolations dependent upon the data chosen and the resultant $\eta(0)$ value quite uncertain. When the data are analyzed in accordance with Eq. (7) on a

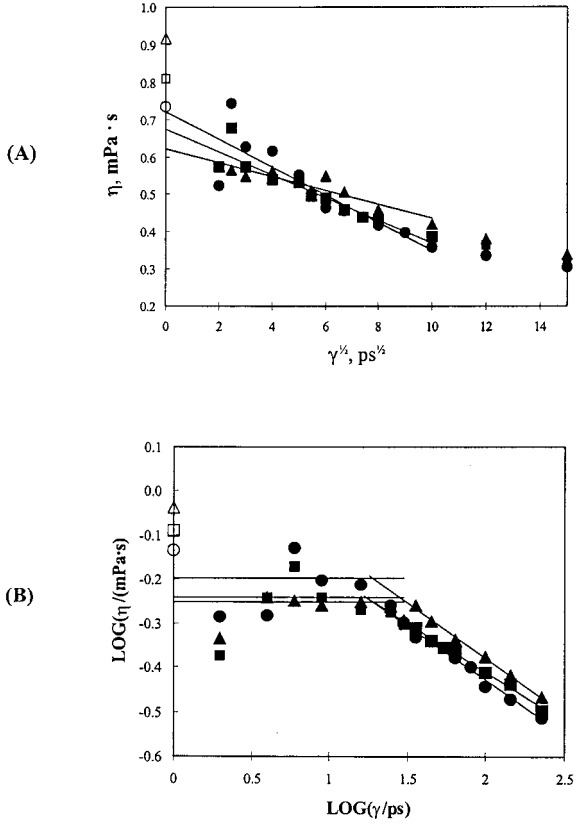

Fig. 5. Simulated viscosities of mixtures containing 70 mol% NBA + 30 mol% IAA (▲), 80 mol% NBA + 20 mol% IAA (■), and 90 mol% NBA + 10 mol% IAA (●) at 35°C and 0.1 MPa, as analyzed using (A) Eq. (5) and (B) Eq. (7) and compared to the experimental values (corresponding open symbols).

log–log plot, they become much more linear in the shear-thinning region, and a definite transition to Newtonian behavior is observed at lower shear rates. Both sets of extrapolated $\eta(0)$ values appear to be lower than the experimental values. Finally, the results for mixtures that are mostly NBA (Fig. 5), show considerable scatter even at higher shear rates and are very difficult to analyze in terms of Eq. (5). The $\eta(\gamma)$ data in Fig. 5A even exhibit what is probably an unreal crossing behavior for the three compositions, an artifact that is essentially rectified when the data are plotted on a log–log plot. However, the viscosity plateaus that appear in Fig. 5B are somewhat ambiguous due to the noise at the lower shear rates, and the $\eta(0)$ values are more difficult to obtain than at lower NBA compositions.

Table IV summarizes the $\eta(0)$ results obtained from the two different extrapolation methods and compares the final values to experimental results. Generally, extrapolation via Eq. (5) yielded results in closer agreement to the experimental values. The average absolute deviations (AAD) for the eleven systems is 12.3% using Eq. (5) and 21.2% using Eq. (7); the biases are -9.4% and -18.5%, respectively.

4. CONCLUSIONS

Our results suggest that the most consistent extrapolation method for obtaining $\eta(0)$ from NEMD simulations is to perform enough long and large simulations to identify clearly the break in $\eta(\gamma)$ data at lower shear rates on a log–log plot. $\eta(0)$ is then obtained in accordance with Eq. (7). In the cases studied here, that of mixtures of polar fluids, a low-shear Newtonian plateau was identifiable from the data when analyzed in this manner. The data in the shear-thinning region were monotonic with respect to composition and more linear than when analyzed using Eq. (5). Analysis using Eq. (5) leads to ambiguities in $\eta(0)$, depending upon the range of γ used, and in clearly identifying a linear region over which the extrapolation is meaningful. Moreover, deviations from linearity when using Eq. (5), curvature even in the shear-thinning regime, is dependent upon the system and model structure.

While the simulated values at low shear were in better agreement with experimental data when analyzed using Eq. (5) instead of Eq. (7), both methods showed considerable negative bias indicating a systematic error due to inadequacies in the model. In a previous study of model effects on viscosity [12], it was found that rigid models produce slightly higher viscosities than models that include potentials associated with vibrations and angle bending. The same study showed that UA models underpredict viscosities while AA models, explicitly including hydrogen atoms as interacting sites, overpredict viscosities when using transferrable LJ parameters for

the groups. This suggests that the negative bias results from additional drag on the hydrogen atoms that is not properly accounted for by the UA model when its parameters are regressed from equilibrium properties. It is of interest in future work to see if a different set of UA parameters for CH_x groups, derived from viscosity data, still produces a negative bias for both analysis methods. It may be that results with a more effective potential model would remove the bias observed here, making the viscosity plateau method quantitatively more accurate in addition to being more consistent and theoretically justified.

ACKNOWLEDGMENT

Support of this project by Neste Oil Company, Espoo, Finland, is gratefully acknowledged.

REFERENCES

1. R. Edberg, G. P. Morriss, and D. J. Evans, *J. Chem. Phys.* **86**:4555 (1987).
2. G. P. Morriss, P. J. Davis, and D. J. Evans, *J. Chem. Phys.* **94**:7420 (1991).
3. A. Berker, S. Chynoweth, U. C. Klomp, and Y. Michopoulos, *J. Chem. Soc. Faraday Trans.* **88**:1719 (1992).
4. S. Chynoweth and Y. Michopoulos, *Mol. Phys.* **81**:133 (1994).
5. R. L. Rowley and J. F. Ely, *Mol. Phys.* **72**:831 (1991).
6. R. L. Rowley and J. F. Ely, *Mol. Phys.* **75**:713 (1992).
7. P. J. Daivis, D. J. Evans, and G. P. Morriss, *J. Chem. Phys.* **97**:616 (1992).
8. M. Lahtela, M. Linnolahti, T. A. Pakkanen, and R. L. Rowley, *J. Chem. Phys.* **108**:2626 (1998).
9. P. Padilla and S. Toxvaerd, *J. Chem. Phys.* **97**:7687 (1992).
10. S. T. Cui, S. A. Gupta, P. T. Cummings, and H. D. Cochran, *J. Chem. Phys.* **105**:1214 (1996).
11. M. Lahtela, T. A. Pakkanen, and R. L. Rowley, *J. Phys. Chem. A* **101**:3449 (1997).
12. W. Allen and R. L. Rowley, *J. Chem. Phys.* **106**:10273 (1997).
13. M. P. Allen and D. J. Tildesley, *Computer Simulation of Liquids* (Clarendon, Oxford, 1987).
14. D. R. Wheeler, N. G. Fuller, and R. L. Rowley, *Mol. Phys.* **92**:55 (1997).
15. P. T. Cummings and T. L. Varner, Jr., *J. Chem. Phys.* **89**:6391 (1988).
16. S. Balasubramanian, C. J. Mundy, and M. L. Klein, *J. Chem. Phys.* **105**:11190 (1996).
17. N. G. Fuller and R. L. Rowley, *Int. J. Thermophys.* **19**:1039 (1998).
18. D. R. Wheeler and R. L. Rowley, *Mol. Phys.* **94**:555 (1998).
19. M. E. Van Leeuwen, *Mol. Phys.* **87**:87 (1996).
20. J. M. Brigs, T. B. Nguyen, and W. L. Jorgenesen, *J. Phys. Chem.* **95**:3315 (1991).
21. D. J. Evans and G. P. Morriss, *Comput. Phys. Rep.* **1**:297 (1984).
22. R. Edberg, D. J. Evans, and G. P. Morriss, *J. Chem. Phys.* **84**:6933 (1986).
23. DIPPR Chemical Database Web Version, http://dippr.byu.edu (1999).
24. M. Thayumanasundaram and P. B. Rao, *J. Chem. Eng. Data.* **16**:323 (1971).